Thickness dependence of exchange anisotropy of polycrystalline Mn3Ir/Co-Fe bilayers

doi: 10.1063/1.1850858

Thickness dependence of exchange anisotropy of polycrystalline Mn_3Ir/Co-Fe bilayers

Ken-ichi Imakita and Masakiyo Tsunoda[a)]
Department of Electronic Engineering, Graduate School of Engineering, Tohoku University, Aobayama 6-6-05 Sendai 980-8579, Japan

Migaku Takahashi
Department of Electronic Engineering, Graduate School of Engineering, Tohoku University, Aobayama 6-6-05 Sendai 980-8579, Japan and New Industry Creation Hatchery Center, Tohoku University, Aobayama 6-6-10, Sendai 980-8579, Japan

(Presented on 9 November 2004; published online 13 May 2005)

The dependence of exchange anisotropy of polycrystalline $Mn_3Ir/Co_{70}Fe_{30}$ bilayers on the antiferromagnetic layer thickness (d_{AF}) was investigated. The degree of order of a Mn–Ir layer in the examined bilayers was almost constant of 0.45, regardless of d_{AF}. The findings are stated as follows. A maximum unidirectional anisotropy constant (J_K) of 1.3 erg/cm^2 is obtained at $d_{AF}=10$ nm. The critical thickness of d_{AF}, where J_K becomes half of its maximum value, is less than 5 nm and comparable to that of the bilayer with disordered Mn–Ir. The blocking temperature (T_B) is enhanced in several-ten degrees with ordering of the Mn–Ir layer. © *2005 American Institute of Physics*. [DOI: 10.1063/1.1850858]

To achieve ultrahigh recording density in hard disk drives (HDDs), the reduction of total thickness of spin valves (SVs) is indispensable because of narrowing read gap of reproducing heads. Therefore, the antiferromagnetic (AFM) layer, whose thickness is dominant in the total thickness of SVs, should be thinner without degrading exchange-biasing properties. A Mn–Ir/Co–Fe bilayer system is a promising candidate to realize very-thin SVs because of its large unidirectional anisotropy constant (J_K) with very thin AFM layer thickness.[1,2] For example, in $Mn_{75}Ir_{25}/Co_{70}Fe_{30}$ bilayer, $J_K=0.87$ erg/cm^2 is obtained with a 5-nm-thick Mn–Ir layer.[3] A remaining problem to be solved for the Mn–Ir/Co–Fe bilayer system is its lower blocking temperature (T_B) than that of the bilayer sytem with PtMn,[4,5] usually used in HDDs.

Recently, the present authors obtained a high blocking temperature of 360 °C, which is comparable to the PtMn system, with a giant J_K of 1.3 erg/cm^2 in Mn–Ir/$Co_{70}Fe_{30}$ bilayers containing Mn_3Ir phase with 10-nm-thick AFM layer.[6] It is quite hopeful if the needed AFM layer thickness is thin enough for the future ultrahigh density HDD heads. We thus investigated the thickness dependence of exchange biasing properties of Mn_3Ir/Co–Fe bilayers in the present study, in connection with the microstructual characterization of the bilayers. In particular, the degree of order was investigated in detail, since it is known to affect strongly on the exchange anisotropy.[7]

The specimens were deposited on thermally oxidized Si wafers with the design of sub./$Cr_{66}Ni_{24}Fe_{10}$5 nm /Cu 50 nm/ $Mn_{73}Ir_{27}d_{AF}$ /$Co_{70}Fe_{30}$4 nm/Cu 1 nm/ Cr–Ni–Fe 2 nm by using magnetron sputtering method. The ultimate pressure of the sputtering chamber was less than 3×10^{-11} Torr and ultra clean Ar (9 N) was used as the sputtering gas. The thickness of the Mn–Ir layer d_{AF} was changed from 5 to 20 nm. During the deposition, except for the Mn–Ir layer, the substrates were held at room temperature (RT). A dc magnetic field of 30 Oe was always applied in the film plane. In order to obtain a template with a flat surface for the epitaxial growth of face-centered-cubic (fcc) Mn–Ir, the 50-nm-thick Cu underlayer was heated at 250 °C for 10 min by using an infrared lamp heater, under the vacuum less than 3×10^{-10} Torr, after its deposition on the Cr–Ni–Fe layer without breaking vacuum. The crystallographic orientation of the Cu layer obtained was well-defined out–of–plane ⟨111⟩-fiber texture, and its surface roughness (R_a) determined from the atomic force microscopy, was 0.38 nm (Ref. 8). Once cooling down the Cu underlayer to RT, the Mn–Ir layer was deposited on it at the respective substrate temperature $T_{sub}=130$ °C–170 °C, and RT for the reference. The Co–Fe layer and the remaining capping layers were further deposited on the Mn–Ir layer, after cooling down the substrate to RT. After breaking vacuum, in order to induce exchange bias to the Co–Fe layer, specimens were annealed in vacuum less than 5×10^{-6} Torr, at $T_a=250$ °C–400 °C for 1 h and were then cooled to RT in a magnetic field of 1 kOe along the same direction to the applied field during the deposition. The field annealing was performed successively on the same specimens.

The microstructure of the films was examined by x-ray diffraction (XRD) and grazing incident x-ray diffraction (GID) with a Cu–$K\alpha$ radiation source. *MH* loops were measured with vibrating sample magnetometer. All the measurement were performed at RT. Unidirectional anisotropy constant J_K was calculated with the equation of $J_K=M_S\cdot d_F\cdot H_{ex}$, where $M_S\cdot d_F$ is the areal saturation magnetization of the Co–Fe layer, and H_{ex} is the exchange biasing field determined as a shift of the center of *MH* loop along the field axis.

Figure 1 shows J_K of the bilayers having various d_{AF} fabricated with $T_{sub}=$RT and 170 °C, as a function of the

a)Electronic mail: tsunoda@ecei.tohoku.ac.jp

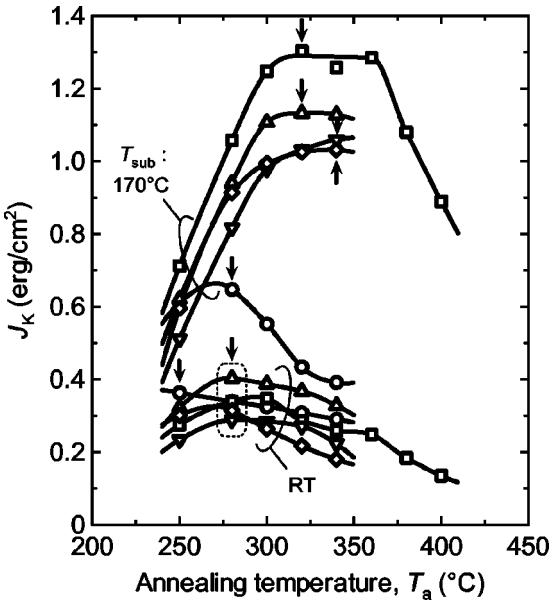

FIG. 1. Changes of J_K of Mn–Ir d_{AF}/Co–Fe 4 nm bilayers fabricated with T_{sub}=170 °C and room temperature (RT) as a function of the annealing temperature, T_a. d_{AF}=5 nm (circle), d_{AF}=7.5 nm (triangle), d_{AF}=10 nm (square), d_{AF}=15 nm (reversed triangle), and d_{AF}=20 nm (diamond), respectively. Arrows indicate the temperature where the respective bilayer shows the maximum J_K value.

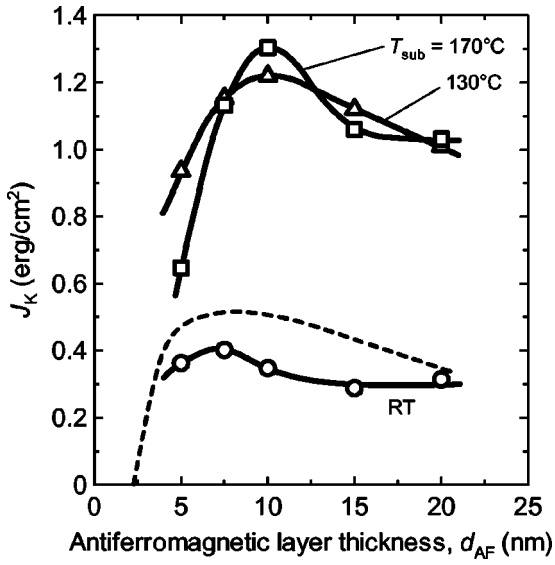

FIG. 2. Changes of J_K of Mn–Ir d_{AF}/Co–Fe 4 nm bilayers fabricated with T_{sub}=130 °C (triangle), 170 °C (square), and room temperature [RT (circle)] as a function of d_{AF}. A dashed line is replotted from Ref. 9, for the similar Mn–Ir/Co–Fe bilayers, which were fabricated on Ta/Ni–Fe/Cu underlayer at T_{sub}=RT and annealed at 300 °C for 0.5 h under 1 kOe.

annealing temperature T_a. The measuring temperature was RT. In the as-deposited state, J_K of all the bilayers were relatively small ($\leqslant$0.1 erg/cm^2), regardless of d_{AF}. However, after the field annealing, J_K drastically changes. For example, in the case of T_{sub}=170 °C with d_{AF}=10 nm, a considerably large value of J_K(=0.71 erg/cm^2) appears at T_a =250 °C, then J_K rapidly increases with increasing T_a and reaches a peak of 1.30 erg/cm^2 at T_a=320 °C (arrowed point). With further increase in T_a>360 °C, J_K steeply decreases. In Fig. 1, the temperature where J_K of the respective bilayer reaches its maximum value is indicated with arrows. We can roughly state that the arrowed temperature rises with increasing either d_{AF} or T_{sub}. This implies that the decrease of J_K observed above the arrowed T_a is probably due to the interdiffusion of the Mn–Ir layer and the Co–Fe layer, and that the elevating substrate temperature is effective to improve the diffusion resistance.

Figure 2 shows the d_{AF} dependence of J_K for the bilayers fabricated with T_{sub}=RT, 130 °C and 170 °C. Here, the achievable J_K value, determined from Fig. 1, was plotted for the respective d_{AF}. A dashed line indicates as a reference the d_{AF} dependence of J_K for the Mn–Ir/Co–Fe bilayers, shown in Ref. 9, which were fabricated on Ta 5 nm/Ni–Fe 2 nm/Cu 5 nm underlayer with T_{sub}=RT and annealed at 300 °C for 0.5 h under 1 kOe. In the case of T_{sub}=RT, J_K shows a similar trend against d_{AF} and a somewhat smaller value in comparison with the dashed line. The cause of the smaller J_K is not clear up to the present, but probably due to the difference of surface structure of the respective Cu underlayers. On the other hand, in the cases of T_{sub}=130 °C and 170 °C, J_K shows a larger value in comparison with both the T_{sub} =RT case and the dashed line, regardless of d_{AF}. Even with d_{AF}=5 nm, a quite large value of J_K=0.94 erg/cm^2 is obtained in the T_{sub}=130 °C case, while the J_K of the T_{sub} =170 °C case is remarkably reduced at d_{AF}=5 nm. Since only the difference between the two cases is the substrate temperature during the deposition of the Mn–Ir layer, the remarkable decrease of J_K at d_{AF}=5 nm in the T_{sub}=170 °C case might be due to the interdiffusion of Mn–Ir and Cu during the deposition process, which results in a reduction of effective Mn–Ir layer thickness. When we define the critical thickness of the antiferromagnetic layer (d_{AF}^{cr}) as the thickness where J_K becomes half of its maximum value, it is less than 5 nm for the T_{sub}=130 °C case and comparable to the cases of T_{sub}=RT and reference. In both cases of T_{sub} =130 °C and 170 °C, J_K decreases with increasing d_{AF} when $d_{AF}\geqslant$10 nm. Although, some possible mechanism for such an inverse proportionality of J_K against d_{AF} is proposed,[10] we now guess that it is due to the insufficient field cooling, namely, lower T_a=320 °C–340 °C than the blocking temperature of the bilayers for thick d_{AF} ($\geqslant$10 nm) cases, as mentioned below.

Figure 3 shows the blocking temperature of the bilayers, appeared in Fig. 2, as a function of the Mn–Ir layer thickness. Here, the T_B is defined as the measuring temperature where J_K vanishes. A dashed line, replotted from Ref. 9, shows the T_B of the same reference bilayers in Fig. 2. The T_B of the bilayer fabricated with T_{sub}=RT shows almost the same value to that of the reference bilayer (dashed line). In contrast, in the cases of T_{sub}=130 °C and 170 °C, the T_B is higher in several-ten degrees than those of the T_{sub}=RT and the reference cases in each d_{AF}. From the viewpoint of spin valve head application for HDDs, these magnetic properties of the bilayer with T_{sub}=130 °C or 170 °C (large J_K, thin d_{AF}^{cr}, and high T_B) are quite favorable.

Figure 4 shows the GID profiles of the bilayers, that appear in Fig. 2. The calculated powder diffraction pattern of Mn_3Ir, having $L1_2$ ordered structure, was also attached at the top of the figure. The conventional θ–2θ scanned XRD profiles show the well-defined out–of–plane fiber texture of the

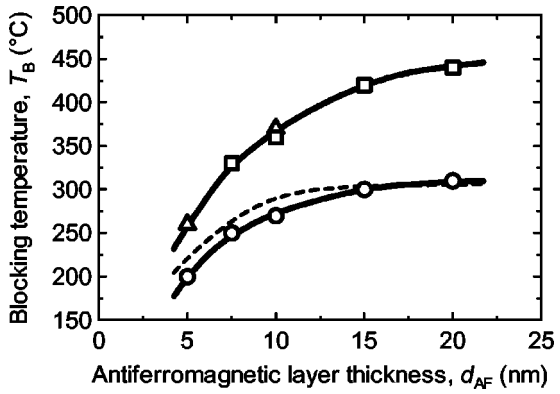

FIG. 3. Changes of the blocking temperature T_B of Mn–Ir d_{AF}/Co–Fe 4 nm bilayers fabricated with T_{sub}=130 °C (triangle), 170 °C (square), and room temperature [RT (circle)] as a function of d_{AF}. A dashed line is replotted from Ref. 9, for the similar Mn–Ir/Co–Fe bilayers, which were fabricated on Ta/Ni–Fe/Cu underlayer at T_{sub}=RT and annealed at 300 °C for 0.5 h under 1 kOe.

bilayers, as ⟨111⟩-texture for the fcc structured Cu and Mn–Ir layers and ⟨110⟩ texture for the body-centered-cubic (bcc) structured Co–Fe layer. Because of the respective texture of the fcc and the bcc layers, we can clearly see the fundamental diffraction line from (220) planes of both the Mn–Ir and Cu layers around $2\theta_\chi$=70 °−75 °, and those from (110) and (200) planes of the Co–Fe layer around $2\theta_\chi$=45 ° and 66° on the respective bilayers. In the case of T_{sub}=RT, only the fundamental diffraction lines are observed in the bilayers for all the d_{AF}. On the other hand, the peaks around $2\theta_\chi$=33 ° and 60°, which correspond to the superlattice diffraction lines from Mn_3Ir (110) and (211), are observed in the case of T_{sub}=170 °C. The degree of order S of the Mn–Ir layer were then determined using the integral intensities ratio of Mn_3Ir (110) peak ($I_{(110)}$) and that of (220) peak ($I_{(220)}$), as follows:

$$S=\sqrt{\frac{I_{(110)}}{I_{(220)}}\frac{(f_{Ir}+3f_{Mn})^2}{(f_{Ir}-f_{Mn})^2}\frac{L(\theta_{\chi(220)})P(\theta_{\chi(220)})\exp\{-2M(\theta_{\chi(220)})\}}{L(\theta_{\chi(110)})P(\theta_{\chi(110)})\exp\{-2M(\theta_{\chi(110)})\}}},$$

where f, L, P, and e^{-2M} are atomic scattering factor, the Lorentz factor, the polarization factor, and the temperature factor, respectively. Here we used the Lorenz factor of $1/\sin 2\theta_\chi$, since the GID profiles were measured for the specimens having strong out–of–plane fiber texture. Figure 5 shows the change of S and the lateral grain size of Mn–Ir layer (D_{220}) in the bilayer that appears in Fig. 2 as a function of the d_{AF}. D_{220} was estimated by using Scherrer's formula[11] from the full width at half maximum of the Mn–Ir (220) diffraction line in the GID profiles. In the case of T_{sub}=RT, S is 0 at all the d_{AF}. In contrast, in the cases of T_{sub}=130 °C and 170 °C, S is almost constant of 0.45, regardless of d_{AF}. The D_{220}, which is 8 nm or 9−10 nm at d_{AF}=5 nm, scarcely increases with increasing d_{AF} and comes to be constant at $d_{AF}\geqslant$10 nm, in both T_{sub} cases. These results mean that the thickness dependence of J_K and T_B, shown in Figs. 2 and 3, are free from the significant influence of the difference of the degree of order and the lateral grain size of the Mn–Ir layer in their qualitative trends. In addition, imperfect ordering of the Mn–Ir layer ($S\sim$0.45) allows us to expect further strong exchange anisotropy, when the S could be 1.0

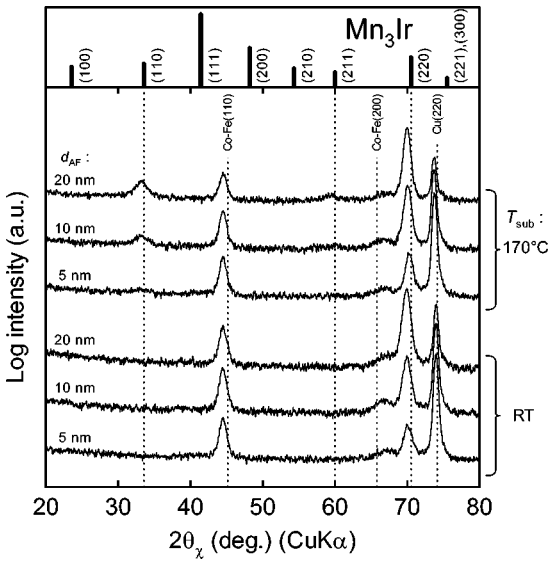

FIG. 4. Grazing incident x-ray diffraction profiles of Mn–Ir d_{AF}/Co–Fe 4 nm bilayers fabricated with T_{sub}=170 °C and room temperature (RT).

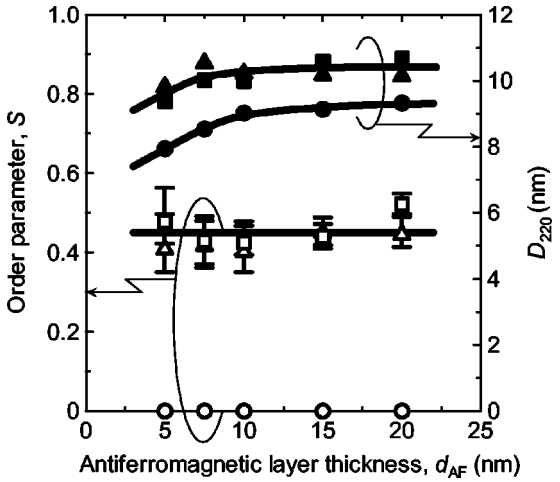

FIG. 5. Changes of the degree of order S (open marks) and lateral grain size D_{220} (solid marks), of Mn–Ir layer, determined with x-ray diffraction technique for the Mn–Ir d_{AF}/Co–Fe 4 nm bilayers fabricated with T_{sub}=130 °C (triangles), 170 °C (squares), and room temperature [RT (circles)] as a function of d_{AF}.

[1]K. Hoshino, R. Nakatani, H. Hoshiya, Y. Sugita, and S. Tsunashima, Jpn. J. Appl. Phys., Part 1 **35**, 607 (1996).
[2]H. N. Fuke, K. Saito, Y. Kamiguchi, H. Iwasaki, and M. Sahashi, J. Appl. Phys. **81**, 4004 (1997).
[3]M. Tsunoda, T. Sato, and T. Hashimoto, Appl. Phys. Lett. **84**, 5222 (2004).
[4]M. Saito, N. Hasegawa, F. Koike, H. Seki, and T. Kuriyama, J. Appl. Phys. **85**, 4928 (1999).
[5]Y. K. Kim, S. R. Lee, S. A. Song, G. S. Park, H. S. Yang, and K. I. Min, J. Appl. Phys. **89**, 6907 (2001).
[6]K. Imakita, M. Tsunoda, and M. Takahashi, Appl. Phys. Lett. **85**, 3812 (2004).
[7]T. Sato, M. Tsunoda, and M. Takahashi, J. Magn. Magn. Mater. **240**, 277 (2002).
[8]K. Imakita, M. Tsunoda, and M. Takahashi, J. Magn. Magn. Mater. **286**, 248 (2005).
[9]M. Tsunoda K. Nishikawa, T. Damm, T. Hashimoto, and M. Takahashi, J. Magn. Magn. Mater. **239**, 182 (2002).
[10]M. Ali, C. H. Marrows, M. Al-Jawad, B. J. Hickey, A. Misra, U. Nowak, and K. D. Usadel, Phys. Rev. B **68**, 214420 (2003).
[11]B. D. Cullity, *Element of the X-Ray Diffraction*, 2nd ed. (Addison-Wesley, Reading. MA, 1978), p. 102.